Low Temperature Physics/Fizika Nizkikh Temperatur, 2021, vol. 47, No. 3, pp. 241–247

Analysis of low-temperature FMR spectra of Fe_3O_4 and $ZnFe_2O_4$ nanoparticles synthesized using organic molecules

K. Yu. Sova, A. S. Vakula, and S. I. Tarapov

O. Ya. Usikov Institute for Radiophysics and Electronics of the National Academy of Sciences of Ukraine
Kharkov 61085, Ukraine
E-mail: katerinesova@gmail.com

A. G. Belous and S. O. Solopan

Institute of General and Inorganic Chemistry of the National Academy of Sciences of Ukraine
Kiev 03142, Ukraine

Received November 11, 2020, published online January 26, 2021

The ferromagnetic resonance (FMR) spectra of Fe_3O_4 and $ZnFe_2O_4$ nanoparticles with organic synthesis products were studied at $T = 4.2$ K. It was determined that the sintering of nanoparticles induced by post-synthesis heat treatment forms a mechanically unstable transition layer between them. Changes in the FMR spectra of Fe_3O_4 nanoparticles synthesized by precipitation in microemulsions using octylphenol ethoxylate and by the cryochemical method are mainly determined by the field of dipole-dipole interaction between nanoparticles.

Keywords: nanoparticles, nanopowders, ferromagnetic resonance, microwave frequencies, low temperatures, organic molecules.

Introduction

Magnetic nanoparticles are a promising material for nanoelectronics and medicine due to the tunable magnetic and resonance properties in the microwave range [1, 2]. Their properties are mainly determined by the forces of magnetic surface anisotropy, magnetocrystalline anisotropy [3–5]. The magnetic dipole-dipole interaction between nanoparticles and magnetoelastic anisotropy field can play an important role when nanoparticles are in the form of nanopowders [6]. Moreover, different methods of their post-synthesis heat treatment affect their magnetic properties and the ferromagnetic resonance (FMR) spectrum although they have the same composition and are prepared by the same synthesis methods [2, 5, 7, 8]. For instance, in Refs. 5, 8, employing FMR spectroscopy in the temperature range of 77–300 K, it is shown what magnetic forces are present in Fe_3O_4 nanoparticles synthesized by different methods using organic molecules before and after heat treatment.

This work compares three types of Fe_3O_4 nanopowders: Fe_3O_4 nanoparticles prepared using diethylene glycol with appropriate metal salts, the same as-prepared nanopowders subjected to post-synthesis separation using a surfactant, the same as-prepared Fe_3O_4 nanopowders after heat treatment in an argon atmosphere. The spectra of the studied nanoparticles differed significantly. At $T < 120$ K, the character of changes of the FMR spectrum was specific. It appeared that a deeper analysis of the FMR spectra of Fe_3O_4 nanoparticles is required at temperatures below 120 K. This will make it possible to determine the magnetic state and to specify processes affecting the magnetic properties and the shape of the FMR spectra of magnetic nanoparticles in the form of nanopowders at low temperatures. It is important to compare the FMR spectra of nanopowders with the replacement of one Fe atom by a nonmagnetic Zn atom. This will allow to detect the factors determining the value of the total anisotropy field H_a at liquid helium temperature.

In our case, it is necessary to take into account the dipole-dipole interaction between nanoparticles, since the nanoparticles are in the nanopowder form, i.e., nanoparticles are combined into conglomerates and chaotically located in the space. Indeed, dipole-dipole interaction is often neglected, assuming that nanoparticles are located at a considerable distance from each other [9]. However, the magnetic dipole-dipole interaction field H_{dip} makes a significant contribution to the total magnetic anisotropy field H_a when the nanoparticles are in the form of a nanopowder [10]. The results obtained from this research are useful in the design of magnetically controlled microwave elements, quantum computing elements, and are also important in the development

© K. Yu. Sova, A. S. Vakula, S. I. Tarapov, A. G. Belous, and S. O. Solopan, 2021

of the targeted drug delivery method. Therefore, it is important to understand how the synthesis method and subsequent processing of magnetic nanoparticles affect their FMR spectra at defferent temperatures; what magnetic interactions will prevail in the studied nanoparticles.

Thus, the aim of this paper is to solve the abovementioned problems by studying the FMR spectra at 4.2 K of Fe_3O_4 and $ZnFe_2O_4$ nanopowders synthesized in aqueous solutions of organic molecules with appropriate metal salts, depending on the method of their post-synthesis treatments.

Theoretical data

FMR was investigated in Fe_3O_4 and $ZnFe_2O_4$ nanopowders based on the study presented in Ref. 11. To describe the shape of the FMR lines, we use the known expression [12]:

$$\chi''(H) = \frac{1}{\pi}\frac{H_r \Delta H_{1/2}\left[\left(H_r^2 + \Delta H_{1/2}^2\right)H^2 + H_r^2\right]}{\left[\left(H - \Delta H_{1/2}\right)^2 H_r^2 + \Delta H_{1/2}^2 H^2\right]\left[\left(H + \Delta H_{1/2}\right)^2 H_r^2 + \Delta H_{1/2}^2 H^2\right]}, \quad (1)$$

where H is the magnitude of the applied external magnetic field; H_r is the resonance field, $\Delta H_{1/2}$ is the halfwidth of the resonance peak.

Let us consider H_r as a function of the total magnetic anisotropy field H_a which mainly depends on the field of the dipole-dipole interaction between nanoparticles H_{dip}, and, to a lesser extent, on the surface anisotropy field H_S, the magnetic crystalline anisotropy field H_K, the external stress field H_σ, and the magnetoelastic anisotropy field H_{el}. Let us determine the largest contribution to H_a among these fields at 4.2 K. Moreover, we also consider H_r as a function of temperature.

The main contribution to H_r is made by the field H_{dip}, which is directly proportional to the magnetization M and inversely proportional to the distance between nanoparticles [3]. The magnetization M for a superparamagnet, including isotropic nanoparticles, is described by the Langevin equation:

$$M = L\left(\frac{\mu H}{kT}\right) \equiv n\mu\left[\coth\left(\frac{\mu H}{kT}\right) - \frac{kT}{\mu H}\right], \quad (2)$$

where L is the Langevin function [2], n is the concentration of nanoparticles, k is the Boltzmann constant. The parameter T is chosen as T = 4.2 K. The parameter H is defined as $H = H_r$ we determine M at each point $H = H_r$ according to the formula (2).

The anisotropy constant k_{eff} is defined by the volume anisotropy constants K_V and the surface anisotropy K_S as

$$k_{eff} = \frac{6K_S}{d} + K_V, \quad (3)$$

where d is the average diameter of the nanoparticle.

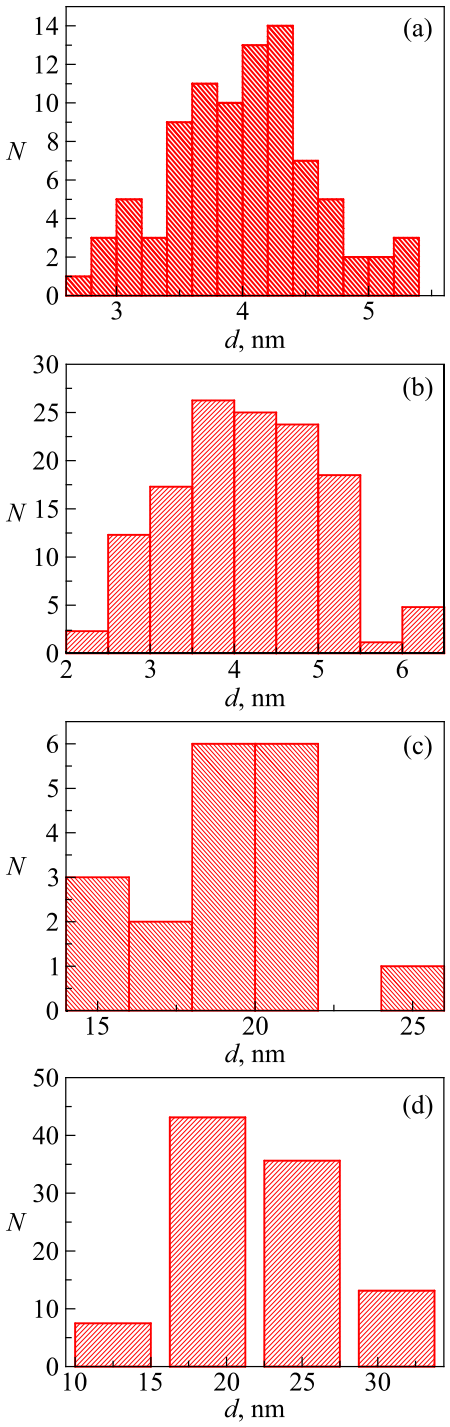

Fig. 1. Size distribution diagrams for Fe_3O_4, $ZnFe_2O_4$ nanoparticles before (a), (b) and after (c), (d) heat treatment.

To find the average diameter of the nanoparticles described in Refs. 11, 13, 14, we used the distribution diagrams shown in Fig. 1. The size distribution diagrams were created based on the analysis of TEM images of the studied nanoparticles using the software Image Tool 3.0.

Diagrams in Fig. 1 show that after heat treatment the average diameter of the studied nanoparticles is shifted to the region of larger values. This indicates a possible fusion of nanoparticles caused by magnetic and van der Waals

forces due to the removal of organic synthesis products, as well as sintering of nanoparticles induced by post-synthesis annealing.

The FMR line shape, taking into account the size distribution of nanoparticles (Fig. 1), is approximated by the model similar to the one presented in Ref. 15.

Experiment and discussion

In our work, we studied Fe_3O_4 and $ZnFe_2O_4$ nanoparticles prepared using diethylene glycol with appropriate metal salts and the same as-prepared nanoparticles subjected to heat treatment. For an additional comparison of the magnetic properties and the FMR spectra, and for the clarification of the role of H_{dip} at low temperatures, we also studied Fe_3O_4 nanoparticles synthesized by cryochemical method and Fe_3O_4 nanoparticles obtained by microemulsion method using Triton X-100 surfactant. Descriptions of the samples are summarized in Table 1.

To control the accuracy of the magnitude of the external magnetic field, 2.2-diphenyl-1-picrylhydrazyl (DPPH) was used as a well-known electron spin resonance reference material. For this material, $g = 2.0036$. We made all the samples in a spherical shape using poly(vinyl butyral)-phenolic (PVB-P) glue for binding.

To study FMR at 4.2 K, we used the experimental research radiospectrometer BURAN (Fig. 2), designed to provide FMR studies in the frequency range of 70–80 GHz, using magnetic fields up to 7 T [16].

An open semi-confocal cavity, which includes a set of the mirrors of different radius of curvature, was used as a measuring cell of the radiospectrometer (Fig. 3).

We placed the studied samples on one of the cavity mirrors. The external magnetic field vector was directed from mirror to mirror.

Typical FMR curves of Fe_3O_4 nanoparticles are shown in Fig. 4.

Based on the obtained experimental FMR data, microwave field frequency f of Fe_3O_4 and $ZnFe_2O_4$ nanoparticles, frequency dependences on the magnitude of the resonance field H_r were determined (Fig. 5).

Fig. 2. Photograph of the experimental research radiospectrometer BURAN.

Fig. 3. Set of mirrors with the different radius of curvature for two-mirror open cavity in the radiospectrometer BURAN.

Table 1. Parameters of the studied samples

Sample number	Chemical formula	Synthesis method	Average nanoparticle size, nm
#1	Fe_3O_4	Precipitation in diethylene glycol at 210 °C [7, 13]	6.9
#2	Fe_3O_4	Precipitation in diethylene glycol at 210 °C, annealed at 500 °C in atmosphere of argon [13]	20–30
#3	$ZnFe_2O_4$	Precipitation in diethylene glycol at 210 °C [13, 14]	3–6
#4	$ZnFe_2O_4$	Precipitation in diethylene glycol at 210 °C, annealed at 500 °C in atmosphere of argon [13, 14]	20–30
#5	Fe_3O_4	Precipitation in microemulsion with organic solvent and using octylphenol ethoxylate (Triton X-100 surfactant) [7]	6.9
#6	Fe_3O_4	Cryochemical synthesis [7]	11

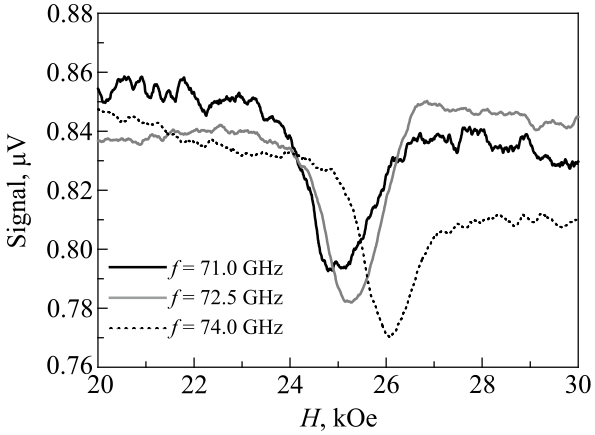

Fig. 4. FMR curves for Fe_3O_4 nanoparticles synthesized by cryochemical method (for several values of the microwave field frequency f).

Black lines in Fig. 5 correspond to the calculated ESR frequency-field dependence for DPPH (calculated ESR line). This line coincides with the experiment with graphical accuracy. As seen in Fig. 5, the experimental points are located on opposite sides of the calculated ESR line for samples #1 and #2. It is caused by the significant difference in H_r. Field $H_a = 1.5$ kOe for sample #1 and $H_a = -0.5$ kOe for sample #2. As expected, the field H_a increases due to an increase in H_{dip} for sample #1. However, the field H_a changes sign after heat treatment.

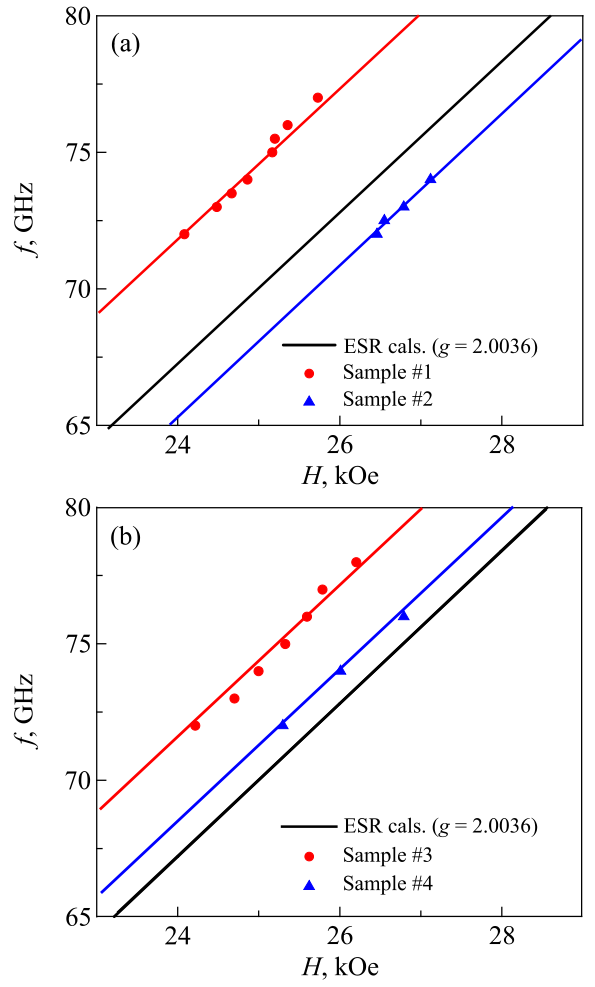

Fig. 5. Dependence of the microwave field frequency f on the external magnetic field $H = H_r$ of Fe_3O_4 (a) and $ZnFe_2O_4$ (b) nanoparticles before and after heat treatment in an atmosphere of argon at 500 °C.

Analysis of the magnetization of samples #1 and #2 [Figs. 6(a), (b)] shows that the value of M increased by 1.8 times after heat treatment in a given range of fields. Removal of organic synthesis products allowed to bind nanoparticles, which significantly increased H_{dip}. However, the difference in the values of the magnetization and, as

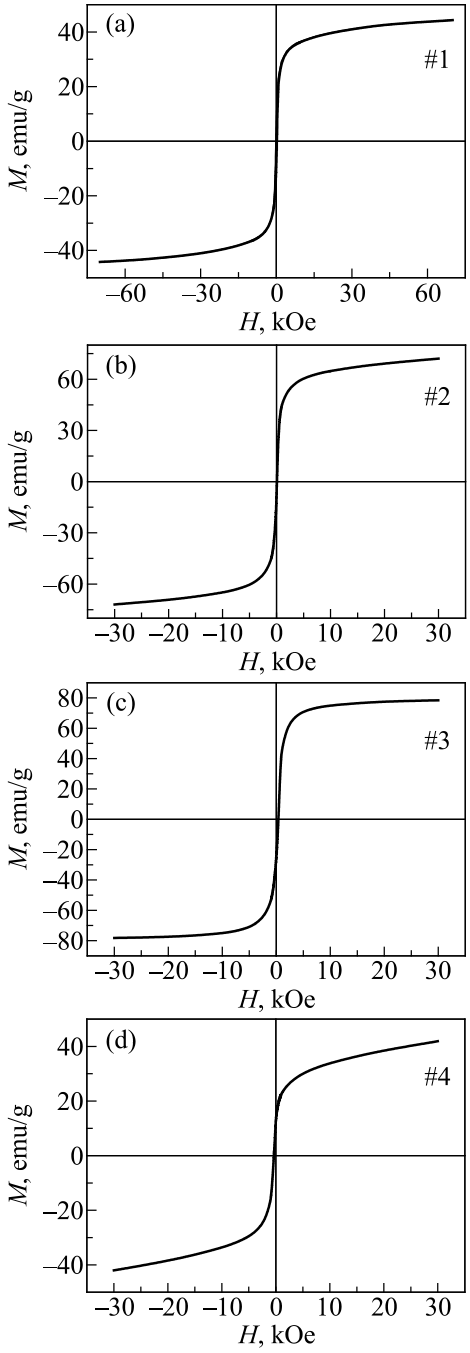

Fig. 6. Magnetic hysteresis loops of Fe_3O_4 and $ZnFe_2O_4$ nanoparticles before (a), (b) and after (c), (d) heat treatment, received at 10 K.

a consequence, the magnitude of the dipole-dipole interaction does not explain the change in the H_a sign.

As for Fe_3O_4, a similar pattern is observed for $ZnFe_2O_4$ nanoparticles (samples #3 and #4): $H_a = 1.1$ kOe for sample #3 and $H_a = 0.4$ kOe for sample #4. However, the sign of the anisotropy field H_a for the latter does not change [Fig. 5(b)]. Note that the M value in the investigated range of FMR fields is lower than for Fe_3O_4 nanoparticles. Therefore, H_a for $ZnFe_2O_4$ is also smaller [Figs. 6(c), (d)].

Heat treatment in an atmosphere of argon leads not only to the removal of synthesis products (i.e., diethylene glycol), but also leads to the sintering of nanoparticles. This sintering changes the shape of the formed nanoparticles and, as a consequence, increases their size, which can be observed from TEM images in Fig. 7.

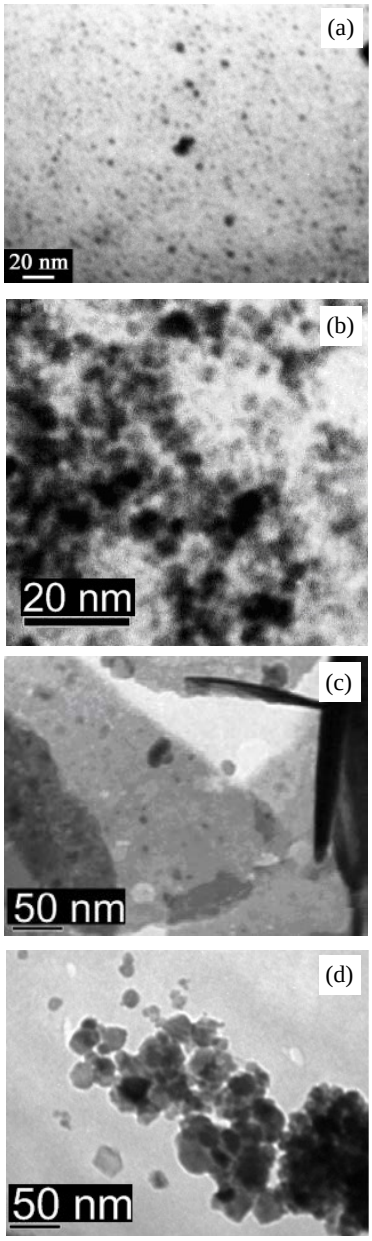

Fig. 7. TEM images of individual Fe_3O_4 and $ZnFe_2O_4$ nanoparticles before (a), (b) and after (c), (d) heat treatment.

The TEM images in Figs. 7(a), (b) clearly show the state of nanoparticles, their size and shape, close to spherical. There is a significant difference in shape and size between nanoparticles before and after heat treatment. Inhomogeneous formations of nanoparticle conglomerates are seen in Figs. 7(c), (d). X-ray structural analysis shows an increase in the intensity of the peaks corresponding to the Fe_3O_4 crystal lattice. The structure of the nanoparticles becomes more like a volumetric material (Fig. 8).

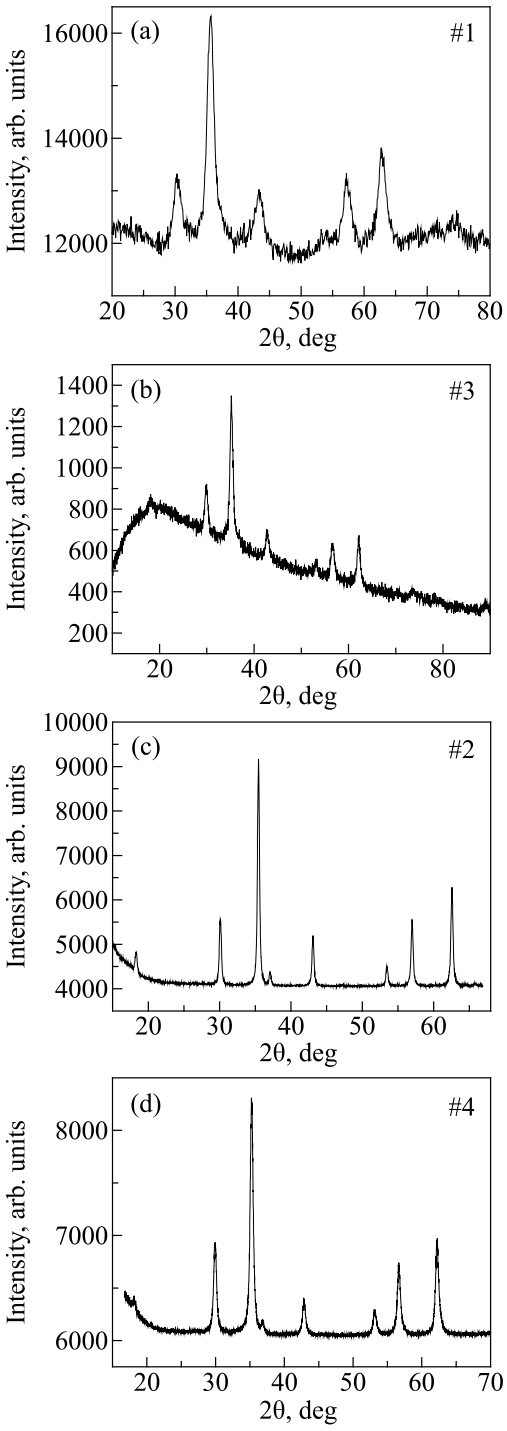

Fig. 8. X-ray diffraction spectra of Fe_3O_4 and $ZnFe_2O_4$ nanoparticles before (a), (b) and after (c), (d) heat treatment.

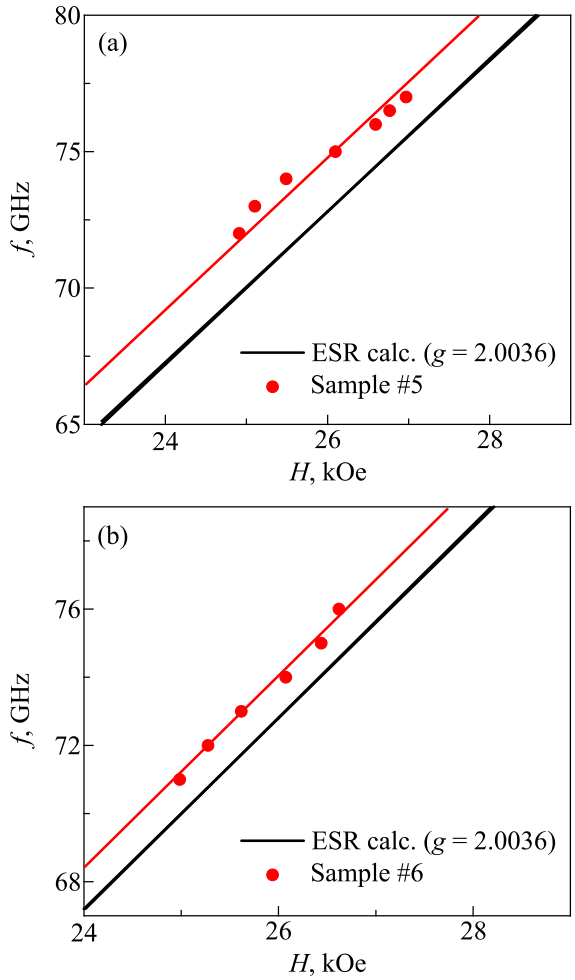

Fig. 9. Dependences of the microwave field frequency f on the external magnetic field $H = H_r$ of Fe_3O_4 nanoparticles synthesized by precipitation in microemulsions using Triton X-100 surfactant (a) and synthesized by cryochemical method (b) at 4.2 K.

Based on the above, it can be considered that sample #2 acquires the properties of the polycrystal with a randomly developed structure. Sintering of nanoparticles occurs due to heat treatment. Most likely, the transition layers are formed as in inhomogeneous ferromagnets (ferrimagnets). However, in the resulting structure, these layers do not have a rigid crystal lattice. Most probably, at low temperatures, mechanical stresses in these layers increase. The resulting additional external stresses field H_σ along with exchange interaction forces in the transition layer (we will use the term "domain wall") can make a sufficiently large contribution to H_a, and this changes its sign.

We have traced a similar pattern for samples #3 and #4. The value H_a also decreases. However, this change is much smaller in compared with changes for Fe_3O_4 nanoparticles. This can be explained by the replacement of one Fe atom by a nonmagnetic Zn atom, which decreases the magnetic interactions in the transition layers. Thereby, the energy of the exchange interaction in the domain wall will be lower than that of Fe_3O_4 nanoparticles [Figs. 6(c), (d)] [17].

To be convinced of the correctness of our assumptions, we studied FMR in Fe_3O_4 nanoparticles synthesized by various methods. For this purpose, we chosen samples #5, #6, synthesized by methods different than samples #1, #2, and studied their properties for further comparison.

We added organic products to sample #5 instead of removing them. Thus, we prevent the binding of nanoparticles, i.e., the formation of conglomerates.

Sample #6 was chosen as a material is inert to temperature changes in the low-temperature range. Nanoparticles for sample #6 were initially synthesized at low temperatures. Therefore, the H_a value will change insignificantly, as shown in [5].

Figure 9 shows the dependences of the resonance field on the frequency of the microwave field for samples #5, #6.

Let us analyze the graphs in Fig. 9. From Fig. 9(a), it is seen that the field H_a also increases at 4.2 K, as for samples #1 and #3. Yet, this increase is not so significant — only by 0.8 kOe. It is related to the fact that surfactant Triton X-100 increases the distance between nanoparticles more than in sample #1. Therefore, the contribution of H_{dip} to H_a is small. At 4.2 K, the magnetization M also increases [Fig. 10(a)], which induced a noticeable increase in H_{dip}. At 300 K, the field H_{dip} can be neglected (on the order of several tens of Oe) [5].

Let us analyze the behavior of sample #6. In the studied temperature range (4.2–300 K), the H_a field stayed almost unchanged (~10 Oe) in comparison with the rest of the samples. Sample #6 shows thermostable properties [Fig. 9(b)].

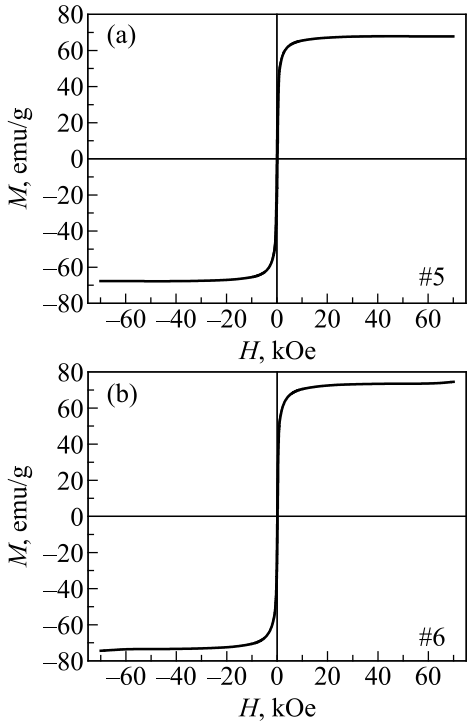

Fig. 10. Magnetic hysteresis loops of Fe_3O_4 nanoparticles synthesized by precipitation in microemulsions using Triton X-100 surfactant (a) and synthesized by cryochemical method (b) at 10 K.

Nanoparticles in sample #6 combine two main factors: temperature of synthesis and the presence of a large number of synthesis products. Due to the first factor, the crystal lattice does not undergo significant changes under the influence of low temperature. Because of the second factor, the nanoparticles in sample #6 weakly interact with each other.

Therefore, the temperature dynamics of nanoparticles after heat treatment is opposite to nanoparticles that were not subjected to heat treatment. For all the samples at 4.2 K, H_{dip} makes the main contribution to the total anisotropy field H_a. It was shown that the field H_{dip} changes in direct proportion to the magnetization M, which is basically a function of temperature [17]. However, at low temperatures in nanoparticles subjected to heat treatment, the influence of the external stress field H_σ arises, the contribution of which to H_a turns out to be competitive with H_{dip}.

Conclusions

This paper presents the results of a study of the magnetic properties of Fe_3O_4 and $ZnFe_2O_4$ nanoparticles synthesized by different methods from organic molecules and subjected to heat treatment. It was found that the total magnetic anisotropy field H_a for each sample is different at 4.2 K. It was shown that the field H_{dip} prevails in all the samples and varies in direct proportion to the magnetization M.

The contributions of dipole-dipole interaction field and magnetic external stress field to the field H_a of the samples before and after heat treatment were analyzed at 4.2 K. It was determined that the arising magnetic forces of the external stresses in the transition magnetic layer of the sintered nanoparticles have a significant influence on H_a and compete with the field H_{dip}. This significantly affects the form of the dependences of the microwave field frequency on the resonance field.

Note that studied nanomaterials are of great importance based on their application in biology, medicine, and nanoelectronics [1, 2]. First of all, this is due to the fact that it is possible to achieve significant changes in the magnetic properties of nanoparticles, depending on the synthesis method. Thus, the above results will be important for monitoring the state of complexes of magnetic nanoparticles with chemotherapeutic drugs in the form of biologically active magnetic fluids. This provides the possibility to determine the efficiency of drug delivery to organs and tissues by changing the FMR spectra. Besides, the studied nanoparticles can be useful in the development of the hyperthermia technique, as nanoparticles administered into tissues must provide the necessary temperature homogeneity in space and time.

1. M. A. Willard, L. K. Kurihara, E. E. Carpenter, S. Calvin, and V. H. Harris, *Int. Mater Rev.* **49**(3–4), 125 (2004).
2. S. P. Gubin, Yu. A. Koksharov, G. B. Khomutov, and G. Yu. Yurkov, *Russ. Chem. Rev.* **74**, 489 (2005).
3. S. Morup, M. F. Hansen, and C. Frandsen, *Beilstein J. Nanotechnol.* **1**, 182 (2010).
4. P. P. Gorbyk, V. N. Myschenko, N. V. Abramov, D. G. Usov, and Yu. N. Troshchenkov, *Surface* **1(15)**, 11 (2009), (in Russian).
5. A. S. Vakula, *Telecommunications and Radio Engineering* **75**, 229 (2016).
6. C. Haase and U. Nowak, *Phys. Rev. B* **85**, 045435 (2012).
7. O. V. Yelenich, S. O. Solopan, T. V. Kolodiazhnyi, J. M. Greneche, and A. G. Belous, *Solid State Phenomena* **230**, 108 (2015).
8. M. Miliaev, A. Vakula, S. Tarapov, A. Belous, and S. Solopan, *Functional Mater.* **26**, 284 (2019).
9. F. Gazeau, J. C. Barcri, F. Gendron, R. Perzynski, Yu. L. Raikher, V. I. Stepanov, and E. Dubois, *JMMM* **186**, 175 (1998).
10. A. S. Vakula, O. A. Kravchuk, S. I. Tarapov, and A. G. Belous, *Radiofiz. Electron.* **25(3)**, 54 (2020).
11. A. Anders, A. Vakula, S. Tarapov, and A. Belous, *Telecommunications and Radio Engineering* **75 (20)**, 1849 (2016).
12. R. B. Morgunov, A. I. Dmitriev, G. I. Dzhardimalieva, A. D. Pomogailo, A. S.Rozenberg, Y. Tanimoto, M. Leonowicz, and E. Sowka, *Phys. Solid State* **49**, 1436 (2007) (in Russian).
13. O. V. Yelenich, S. O. Solopan, V. V. Trachevskii, and A. G. Belous, *Russian Journal of Inorganic Chemistry* **58**, 901 (2013).
14. O. V. Yelenich, S. O. Solopan, T. V. Kolodiazhnyi, V. V. Dzyublyuk, A. I. Tovstolytkin, and A. G. Belous, *Mater. Chem. Phys.* **146**, 129 (2014).
15. T. Kalmykova, A. Vakula, S. Nedukh, S. Tarapov, A. Belous, and O. Yelenich, *Functional Mater.* **23**, 618 (2016).
16. S. I. Tarapov, Y. P. Machekhin, and A. S. Zamkovoy, *Magnetic Resonance for Optoelectronic Materials Investigating*, Collegium, Kharkiv (2008).
17. S. V. Vonsovsky, *Magnetism*, Nauka, Moscow (1971) (in Russian).

Аналіз низькотемпературних спектрів ФМР наночастинок Fe_3O_4 та $ZnFe_2O_4$, синтезованих з використанням органічних молекул

K. Yu. Sova, A. S. Vakula, S. I. Tarapov, A. G. Belous, S. O. Solopan

Проведено дослідження феромагнітного резонансу (ФМР) при $T = 4{,}2$ K в наночастинках Fe_3O_4 та $ZnFe_2O_4$ з органічними продуктами синтезу. За спектрами ФМР визначено, що спікання наночастинок після їх термообробки формує між ними механічно нестійкий перехідний шар. Зміна спектрів ФМР наночастинок Fe_3O_4, які синтезовано осадженням в мікроемульсіях з використанням октілфенола етоксілата та кріохімічним методом, визначаються в основному полем диполь-дипольної взаємодії між наночастинками.

Ключові слова: наночастинки, нанопорошки, феромагнітний резонанс, надвисокі частоти, низькі температури, органічні молекули.